MOLECULAR AND CELLULAR BIOLOGY, Nov. 1996, p. 6363–6371 Vol. 16, No. 11
0270-7306/96/$04.00+0

Differential Regulation of NF-κB2(p100) Processing and Control by Amino-Terminal Sequences

JONATHAN C. BETTS AND GARY J. NABEL*

Departments of Internal Medicine and Biological Chemistry, Howard Hughes Medical Institute, University of Michigan Medical Center, Ann Arbor, Michigan 48109-0650

Received 7 February 1996/Returned for modification 29 March 1996/Accepted 14 August 1996

Proteolytic degradation of the C-terminal region of NF-κB precursors to their active DNA binding forms represents an important regulatory step in the activation of NF-κB. NF-κB2(p100) is found ubiquitously in the cytoplasm; however, the site and mechanism of processing to p52 have not previously been defined. We show by deletion mapping that processing of NF-κB2(p100) terminates at alanine 405 to generate p52 and is prevented by specific inhibitors of the multicatalytic proteinase complex. Although the C-terminal IκB-like domain of NF-κB2(p100) was constitutively phosphorylated, disruption of this phosphorylation by mutagenesis demonstrated that it was not required as a signal to mediate processing. Mutational analysis further showed that cleavage of NF-κB2 is not dependent on a specific sequence motif adjacent to alanine 405, the ankyrin repeats, or other C-terminal sequences but is directed by structural determinants amino terminal to the cleavage site, within the Rel homology domain and/or the glycine hinge region. The level of processing of NF-κB2(p100) was much lower than that of NF-κB1(p105) and differed from that of IκB-α, suggesting differential control of processing of NF-κB/IκB family members.

Many genes which are induced during immune and inflammatory responses contain an important *cis*-acting regulatory sequence in their enhancers which binds members of the NF-κB family of transcription factors. Such genes include inflammatory cytokines and their receptors, adhesion molecules, major histocompatibility complex molecules, acute-phase proteins, and viral enhancers such as the human immunodeficiency virus long terminal repeat (reviewed in references 48 and 50). The NF-κB family comprises a number of gene products [NF-κB1, NF-κB2, RelA(p65), RelB, and c-Rel in mammals] which have the capacity to form a variety of homo- and heterodimers through the 300-amino-acid Rel homology domain (RHD). The importance of these proteins is suggested by the evolutionary conservation of this domain in distantly related species, including *Drosophila melanogaster*, in which the Rel-related proteins Dif and dorsal are found (22, 49). Indeed, while the proteins are functionally interdependent, knockout studies of the different loci have demonstrated unique pivotal roles in the inflammatory (NF-κB1) and immune (c-Rel and RelB) responses as well as in development (RelA) (3, 24, 47, 56).

The classical form of NF-κB, a heterodimer of NF-κB1(p50) and RelA(p65) subunits, is maintained as a preformed, inactive cytoplasmic complex through binding to an inhibitory subunit, IκB. Treatment of cells with agonists such as tumor necrosis factor alpha (TNF-α), interleukin-1, and bacterial lipopolysaccharide results in phosphorylation-ubiquitination and degradation of IκB through the proteasome pathway, allowing translocation of transcriptionally active NF-κB to the nucleus (7, 8, 11, 31, 52, 57). Knockout studies also suggest that IκB-α is important in attenuation of nuclear NF-κB activity (2). The temporal and qualitative nature of the response is further regulated by different IκB gene products (α and β [51]). The NF-κB1(p50) and NF-κB2(p52) precursors (p105 and p100, respectively) provide an additional level of control, with specific degradation of the C-terminal ankyrin repeat-containing portion of the molecule being required to unmask the nuclear localization signal and DNA binding domain (21, 26, 41).

The ubiquitin-proteasome pathway is important in the regulation of many proteins within the cell through targeted degradation (10). Recently this pathway has been shown to modulate specifically the activities of a number of molecules, including cell cycle regulators (e.g., cyclins [40]), integral membrane proteins (23, 55), transcription factors such as Jun (54), and IκB proteins (8, 37, 53). In addition, the proteasome has been implicated in the processing of peptides for presentation by the major histocompatibility complex with gamma interferon treatment, resulting in alteration in the subunit structure and, hence, specificity of the proteasome (17, 42). While proteins which enter the proteasome are generally completely degraded to short peptides, NF-κB precursors are unusual, since proteolysis is terminated within the molecule, leaving the N terminus intact. How this termination is mediated is at present unknown. In this report, we examine the proteolysis of NF-κB2(p100) (4, 34, 46) to p52, define its processing site, and characterize the structural components which determine the site of processing and render the RHD resistant to proteasome activity.

MATERIALS AND METHODS

Materials. A protease inhibitor, *N*-benzyloxycarbonyl-Ile-Glu(*O*-*t*-butyl)-Ala-leucinal (PSI), was the generous gift of Sherwin Wilk, Mt. Sinai Medical Center (15, 58). Rabbit polyclonal antisera were as follows: anti-p100N (αp100N) was raised against the N-terminal 18 residues of NF-κB2 (45), αp105N (Ab1141) was raised against the N terminus of NF-κB1 (a generous gift of Nancy Rice, National Institutes of Health [41]), and αRelA(p65) (sc-109) was obtained from Santa Cruz Biotechnology, Inc., Santa Cruz, Calif. λ phosphatase (λ-PPase) was obtained from New England Biolabs, Inc., Beverly, Mass. TNF-α was from Genzyme, Cambridge, Mass. *N*-Tosyl-L-phenylalanine chloromethyl ketone (TPCK) was obtained from Sigma Chemical Co., St. Louis, Mo.

Cell lines. All cell lines utilized were human in origin and maintained in log phase. 293 cells (E1A-transformed kidney epithelium) and HeLa (cervical carcinoma) were maintained in Dulbecco's modified Eagle medium containing 10% fetal bovine serum, 50 U each of penicillin and streptomycin per ml, and 50 μg of L-glutamine per ml. 293 transfections were carried out by the calcium phos-

* Corresponding author. Mailing address: Howard Hughes Medical Institute, Departments of Internal Medicine and Biological Chemistry, University of Michigan Medical Center, 1150 W. Medical Center Dr., 4520 MSRB I, Ann Arbor, MI 48109-0650. Phone: (313) 647-4798. Fax: (313) 647-4730.

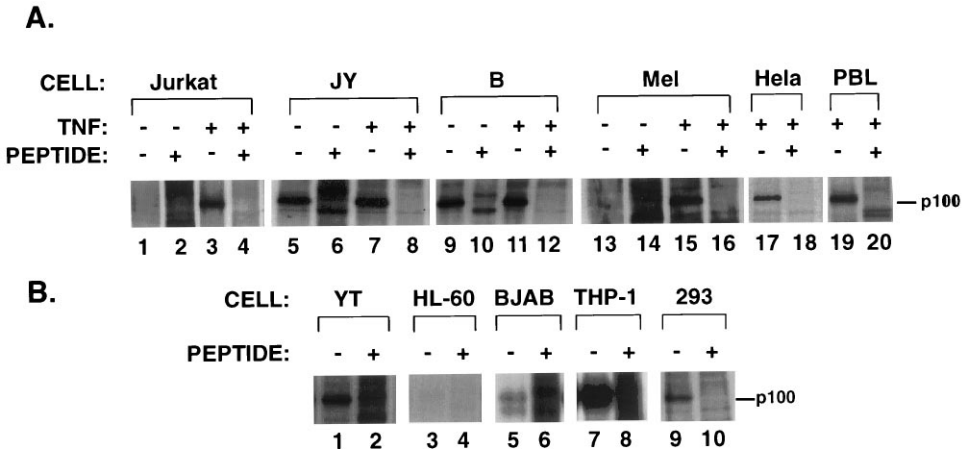

FIG. 1. Expression of NF-κB2(p100). (A) NF-κB2(p100) is widely expressed. NF-κB2(p100) was immunoprecipitated from Jurkat, JY, UM-291 B, UM-449 melanoma (Mel), HeLa, and peripheral blood T cells (PBL) following labeling with [^{35}S]Met-Cys for 6 h in the absence or presence of 200 U of TNF-α per ml for 4 h as shown. (B) The cell types shown were labeled for 12 h with [^{35}S]Met-Cys prior to immunoprecipitation with αp100N. A peptide immunogen was added to the reaction mixtures in the even-numbered lanes to demonstrate the specificity of the complexes detected. The position of the p100 band is indicated. Equivalent exposures for each cell type are shown and hence reflect relative protein levels.

phate procedure as described previously (38). Jurkat T leukemia cells were grown in RPMI 1640 medium with 5% fetal bovine serum. JY cells, UM-291 cells (Epstein-Barr virus-transformed B cells generated by established methods in the University of Michigan Core Immortalization Laboratory), BJAB B cells, YT (natural killer) cells, HL-60 (promyelocytic) cells, and UM-449 melanoma cells were maintained in RPMI 1640 containing 10% fetal bovine serum. THP-1 (monocytic leukemia) cells were grown in the latter medium supplemented with 20 μM 2-mercaptoethanol. Peripheral blood leukocytes were isolated by Ficoll gradient centrifugation and maintained in RPMI 1640 with 10% human AB serum.

Plasmids. NF-κB2(p100) was cloned into pRc/RSV (Invitrogen Corp., San Diego, Calif.) to generate RSV-p100 with transcription directed by the Rous sarcoma virus (RSV) long terminal repeat and poly(A) signals from the bovine growth hormone gene. NF-κB1(p105) and NF-κB2(p100) were also expressed from an alternative clone containing the RSV long terminal repeat and simian virus 40 poly(A) sequences as previously described (39, 46) where indicated. The following plasmids were constructed in the latter vector: RSV-100-445, RSV-100-422, RSV-100-406, RSV-100-405, RSV-100-399, and RSV-100-360. These plasmids contained termination codons following Glu-445, Glu-422, Gln-406, Ala-405, Pro-399, and Ser-360 of NF-κB2, respectively. PCR with mutagenic primers was utilized to introduce restriction sites for the construction of the following NF-κB1/NF-κB2 fusion constructs: RSV-NF-κB2/1(400/401), a 969-residue protein with the junction sequence CYPG/TGPG; NF-κB2/1(316/342), 943 residues with the junction sequence RGGD/TSED; and NF-κB1/2(342/318), a 923-residue protein with the junction sequence DLET/SDSK. A termination codon was introduced following alanine 405 of NF-κB2 in RSV NF-κB1/2(342/318) to generate RSV-NF-κB1/2-405, encoding a 430-residue fusion protein. RSV-NF-κB2(449)lacZ and RSV NF-κB2(400)lacZ encode residues 1 to 449 and 1 to 400 of p100, respectively, fused to the C-terminal 518 codons of the *Escherichia coli lacZ* gene. Site-directed mutagenesis was carried out with the Chameleon system (Stratagene, La Jolla, Calif.). In NF-κB2(Δ3S), serines 713, 715, and 717 of NF-κB2 were mutated to Gly, Ala, and Ala, respectively. In RSV-p100ΔDIM, residues 247 to 249 (Tyr, Leu, and Leu) were mutated to alanines. Details of cloning for the constructs described above are available upon request.

Cell labeling and immunoprecipitation. Cells were washed twice in serum-free methionine- and cysteine-deficient medium and starved for 45 min in 1 ml of medium per 10^7 cells prior to treatment with 100 μCi of [^{35}S]Met-Cys (^{35}S-PROMIX in vitro cell labeling mix; Amersham Life Science Inc.) for 30 min. The cells were then washed twice in complete medium and chased for various times with complete medium containing a 100-fold excess of L-methionine. The cells were harvested and washed once in phosphate-buffered saline prior to lysis in immunoprecipitation buffer (137 mM NaCl, 20 mM Tris-Cl [pH 8.0], 0.2 mM EDTA, 10% glycerol, 1% Triton X-100, 1 mM phenylmethylsulfonyl fluoride, 1 μg [each] of leupeptin and aprotinin per ml). When indicated, a more stringent buffer which also contained 0.5% sodium deoxycholate and 0.1% Nonidet P-40 was used. Following incubation on ice for 10 min, lysates were clarified by microcentrifugation for 10 min. The protein content was determined by the Bradford assay. Proteins were immunoprecipitated at 4°C for 4 h with αp100N or αp105N with protein G-agarose beads. The beads were washed three times in 0.5 ml of buffer at 4°C prior to elution by boiling in 50 μl of Laemmli loading buffer and resolution by sodium dodecyl sulfate-polyacrylamide gel electrophoresis (SDS-PAGE). Gels were treated with Autofluor (National Diagnostics, Atlanta, Ga.), dried, and exposed to film or PhosphorImager analysis (Molecular Dynamics). For phosphatase treatment, following immunoprecipitation and washing, the beads were resuspended in 30 μl of 1× λ-PPase buffer and incubated with various concentrations of enzyme at 30°C for 30 min. Loading buffer was added directly to the reaction mixture and boiled before electrophoresis.

Western blot (immunoblot) analysis. Proteins resolved by SDS-PAGE were transferred to nitrocellulose. Blocking, incubation with antibodies, and washing (20 min for each step) were carried out in 20 mM Tris-Cl (pH 7.5)–100 mM NaCl–0.5% nonfat milk–0.3% Tween 20 at room temperature. Peroxidase-conjugated secondary antibodies were utilized to visualize immunoreactivity by chemiluminescence (ECL; Amersham).

RESULTS

NF-κB2(p100) is expressed ubiquitously and is constitutively phosphorylated. NF-κB2(p100) has strong structural homology to NF-κB1(p105); however, the active DNA binding complex in the nuclei of stimulated cells consists largely of NF-κB1(p50)/RelA heterodimers. We undertook a survey of cell lines and found that NF-κB2(p100) was present at various levels in the cytoplasm of all cells studied. Different cell types, including Jurkat T leukemia cells, HeLa cervical epithelial cells, and human melanoma cells, were radiolabeled, and immunoprecipitation of cell lysates was performed with NF-κB2-specific antiserum (αp100N). Although NF-κB2(p100) was not found in several types of unstimulated cells under these conditions, the protein was readily detected after stimulation with TNF-α for 4 h (Fig. 1A). In B-cell lines, including JY, UM-291, and BJAB, and in the monocyte line THP-1, a high constitutive level of NF-κB2(p100) was detectable, but there was no further elevation following TNF-α stimulation (Fig. 1A, lanes 5 to 12, and B, lanes 5 to 8). Increasing the labeling time of cells from 6 to 24 h allowed the detection of NF-κB2(p100) in all cell types (Fig. 1B, lanes 1, 3, 5, 7, and 9). The processed form of NF-κB2, p52, was not readily detectable in these studies; however, we have previously observed that αp100N has reduced avidity for p52 when it is heterodimerized with other Rel family members such as RelA (45).

In some cell types, including the 293 renal epithelial and UM-449 melanoma cell lines, NF-κB2(p100) was evident as a doublet, and treatment of the immunoprecipitated protein with λ-PPase resulted in the disappearance of the upper band of the doublet, whereas the lower p100 and p52 bands were unaffected (Fig. 2A, lane 2 versus lanes 3 and 4). λ-PPase has

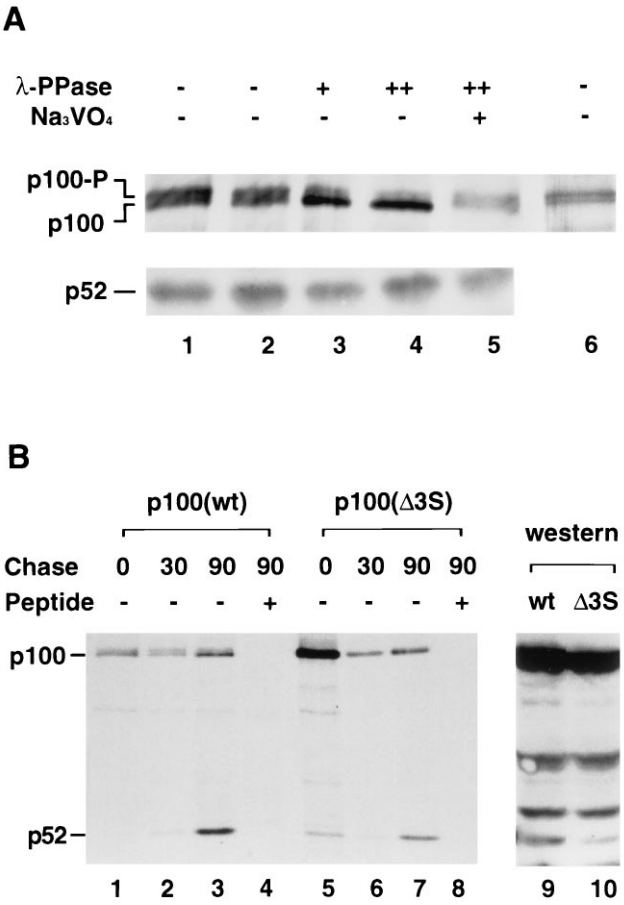

FIG. 2. NF-κB2(p100) is constitutively phosphorylated in the C terminus. (A) ^{35}S-labeled protein immunoprecipitated from 293 cells with αp100N was then incubated as follows: lane 1, no treatment; lane 2, phosphatase buffer alone; lane 3, 40 U of λ-PPase; lane 4, 200 U of λ-PPase; and lane 5, 200 U of λ-PPase plus 10 mM Na_3VO_4. Inhibition of phosphatase activity by orthovanadate (lane 5) indicates that dephosphorylation is occurring and not proteolysis. Treated proteins were eluted by boiling in SDS sample buffer and separated on SDS–6% PAGE. The gel was run for longer than normal in order to clearly distinguish the p100 doublet. A p100 doublet was also observed in the human melanoma cell line UM-449 (lane 6). (B) 293 cells transfected with RSV-100Δ3S lacked the upper phosphorylated form, but the rate of processing to p52 was unaffected. Cells were labeled for 30 min and then chased for 0, 30, or 90 min with excess cold medium. Precursor (p100) and processed (p52) forms are indicated. Lanes 1 to 4, wild-type (wt) NF-κB2(p100); lanes 5 to 8, Δ3S mutant. Lanes 4 and 8 contained the same material as lanes 3 and 7, respectively, but with the addition of an NF-κB2 peptide immunogen competitor to demonstrate specificity of the immunoprecipitated complexes. The steady-state levels of the wild-type and mutated versions of the proteins were comparable as demonstrated by Western blot analysis (lanes 9 and 10).

multiple specificities, including dephosphorylation of serine and threonine residues (59); hence, a number of point mutations were made in these residues throughout the C terminus of NF-κB2(p100). The region between residues 704 and 718 of NF-κB2 was of particular interest because it contains several overlapping casein kinase I and II sites. Three serines were mutated in this region. DSDSDSE (residues 712 to 718) was mutated to DGDADAE to generate RSV-100Δ3S. Following transfection of this mutant into 293 cells, the upper phosphorylated form of p100 was not detected, suggesting that these sites are required for the modifications required to generate the higher-molecular-weight protein. Steady-state levels of wild-type and mutant proteins were equivalent in these studies as determined by immunoblotting (Fig. 2B, lanes 9 and 10), indicating that the mutant does not titrate a basal kinase activity. Although Ser-713 and Ser-715 are within casein kinase II (XS/TXXD/E) consensus sites, the identity of the kinase responsible for phosphorylating this site in NF-κB2 is presently unknown. However, the phosphorylation of NF-κB2(p100) observed here in 293 cells was constitutive, and the Δ3S mutation had no discernible effect on processing (Fig. 2B). In UM-449 cells, p100 was detectable only after cellular stimulation; hence, it is unclear whether the appearance of the hyperphosphorylated form was signal mediated. However, the p100 doublet was not evident in several other cells after TNF-α treatment, including Jurkat, JY, UM-291, YT, BJAB, and HeLa cells and primary peripheral blood leukocytes, indicating that this is unlikely to be a general TNF-α-mediated event.

NF-κB2(p100) proteolysis is prevented by inhibitors of the multicatalytic proteinase complex. NF-κB2(p100) and NF-κB1 (p105) have highly conserved structural motifs throughout the molecules. These motifs include the N-terminal RHDs nuclear localization sequence, glycine hinge, ankyrin repeats, and C-terminal PEST-like sequences; however, there are significant differences between the primary sequences of the C termini of the two molecules downstream of the glycine hinge. In order to characterize NF-κB2(p100) processing, transfected 293 cells were metabolically labeled, and the generation of the processed form, p52, was monitored by pulse-chase analysis. p52 was detectable after a 30-min chase period and increased with time such that ~10% of the labeled protein was processed after 5 h. In contrast, the rate of processing was ≥5-fold higher for NF-κB1 than for NF-κB2, with 10% of the labeled protein being converted to p50 by 1 h (Fig. 3A). While the molecules in these experiments were predominantly NF-κB2 homodimers, we found no differences in the rate of processing of p100 when it was dimerized with other Rel family members, such as RelA or NF-κB1(p50) (data not shown).

Peptide aldehyde inhibitors of the multicatalytic proteinase complex, or proteasome, have been demonstrated to prevent the proteolysis of NF-κB1(p105) and the signal-induced degradation of IκB-α (8, 37, 53). PSI specifically inhibits the chymotrypsin- and calpain-like activities of the multicatalytic proteinase complex with minimal effect on other cellular proteases, including trypsin-like peptidylglutamyl peptide and small neutral amino acid-preferring activities (58). Treatment of 293 cells with PSI resulted in a dramatic inhibition of NF-κB2(p100) processing, with half-maximal inhibition at 0.1 μM (Fig. 3B, lanes 2 to 5). When the effect on NF-κB1 proteolysis was investigated, processing was not inhibited at this concentration (Fig. 3B, lane 7) but required doses of 7 μM to achieve half-maximal inhibition. Similar results were obtained with another peptide aldehyde, MG-132, a specific inhibitor of the 26S proteasome (37, 42) (data not shown). Other inhibitors of IκB-α degradation, including the chloromethyl ketones TPCK and *N*α-*p*-tosyl-L-lysine chloromethyl ketone (TLCK) and *N*-acetyl-DL-Phe-β-naphthylester (APNE) (20), had no effect on p100 processing at concentrations of up to 200 μM (Fig. 3B, lanes 11 to 13). Interestingly, these latter compounds have recently been shown to nonspecifically inhibit the phosphorylation step of IκB-α inactivation rather than proteolysis per se (16). These data support a role for the multicatalytic proteinase complex in NF-κB2(p100) proteolysis and further suggest differential control of the processing of NF-κB and IκB family members.

Proteolysis of NF-κB2(p100) terminates at alanine 405. The processed form of NF-κB2 has an apparent molecular mass of 52 kDa as determined by denaturing SDS-PAGE. We had previously created deletion mutants to generate such a truncated protein by introducing a stop codon at the *Xho*I site of p100; however, this protein had a significantly lower mobility

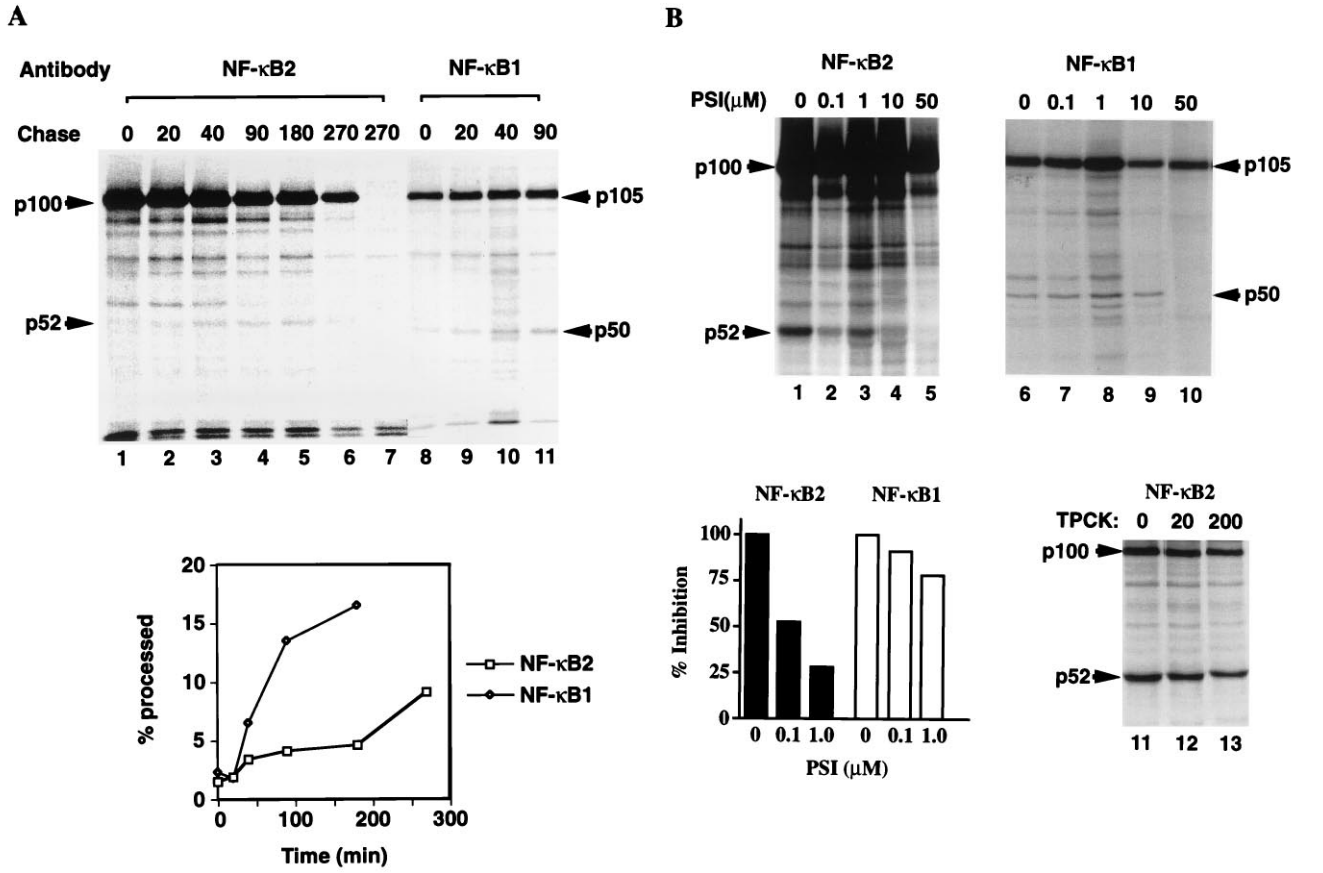

FIG. 3. Comparison of NF-κB2(p100) and NF-κB1(p105) processing. (A) Transfected 293 cells were labeled with [^{35}S]Met-Cys for 30 min and chased for the indicated times with unlabeled amino acids prior to lysis and immunoprecipitation with NF-κB2- or NF-κB1-specific antibodies. Lane 7 contains a p100N peptide competitor. Precursor and processed forms were quantitated with a PhosphorImager and plotted as the percentage of counts in the processed form versus time. (B) A multicatalytic proteinase complex inhibitor inhibits NF-κB2 proteolysis. Transfected 293 cells were labeled for 30 min and chased for 90 min prior to the preparation of extracts and immunoprecipitation with αp100N (lanes 1 to 5) or αp105N (lanes 6 to 10). The indicated concentrations of PSI were present during the starvation, labeling, and chase periods. Other inhibitors of IκB-α degradation, for example, TPCK at doses of 20 and 200 μM (lanes 12 and 13), had no effect on NF-κB2 proteolysis. Control lanes contained dimethyl sulfoxide vehicle alone (lanes 1, 6, and 11). The gels shown were run at different times, and hence the distances migrated in the three gels are not relative. The graph shows the levels of processing following treatment with various doses of PSI, expressed as percentages of the untreated level.

by SDS-PAGE (apparent molecular mass of ~60 kDa), suggesting that cleavage normally occurred N terminal to this predicted site. A series of deletions which terminated NF-κB2 at Glu-445, Glu-422, Gln-406, Ala-405, Pro-399, and Ser-360 was constructed. Following transfection into 293 cells, the migration of each protein was determined after separation of extracts by SDS-PAGE and immunodetection with αp100N (Fig. 4A). The R_f values were determined and demonstrated a linear correlation with the number of amino acid residues in the truncated protein, and the naturally processed protein comigrated with the deletion mutant which terminated at Ala-405 (Fig. 4A, lane 5; Fig. 4B). The calculated molecular mass of NF-κB2 truncated at Ala-405, on the basis of amino acid composition, is only 44 kDa, which is significantly lower than the apparent 52 kDa. We have detected no secondary modification of the N terminus of NF-κB2 (by using phosphatases, glycosidases, lipases, and reduction-alkylation) which is likely to cause this molecular mass shift (data not shown), and we suggest that conformational determinants of the RHD are responsible for the observed mobility in SDS-PAGE.

Resistance of the N-terminal regions of NF-κB precursors to proteolysis. The C terminus of NF-κB2(p100) is thus specifically degraded by the proteasome and terminates at Ala-405, C terminal to the RHD. To characterize the sequence which prevents processing of this N-terminal region, we examined the proteolysis of a series of NF-κB1/NF-κB2 fusion proteins. A fusion protein, NF-κB2/1(316/342), containing NF-κB2 sequences 1 to 316 fused to the nuclear localization sequence, glycine hinge, and ankyrin repeats of NF-κB1, was made (Fig. 5A). When this protein was processed in 293 cells, a product with the same mobility as p52 was detected (Fig. 5B, lane 2 versus lane 4). Conversely, NF-κB1/2(342/318) generated a processed product with the same mobility as p50 (Fig. 5B, lane 6 versus lane 8). To determine whether processing terminated at the same point in NF-κB1/2(342/318) as in wild-type NF-κB2 (i.e., Ala-405), a stop codon was introduced following Ala-405 in NF-κB1/2(342/318) to generate NF-κB1/2(405stop). The protein expressed by the latter construct had an identical mobility of 50 kDa (Fig. 5C, lane 3), demonstrating that processing terminated at the same residue as in wild-type NF-κB2 (p100).

This result suggested that proteolysis occurred at Ala-405 of NF-κB2 in both native and chimeric proteins, but it was unclear whether it was the location in the molecule or the primary sequence at this site which was important for determining the site of processing. To define this region, a fusion protein, NF-κB2/1(400/401), was generated, in which the sequence immediately surrounding Ala-405 was deleted and the C terminus

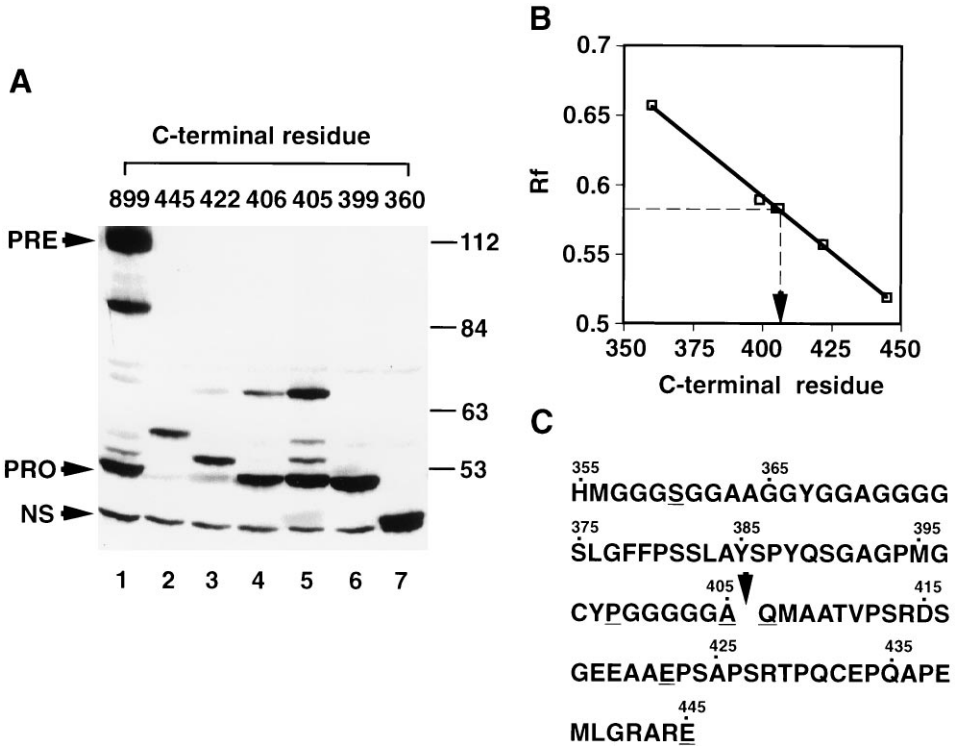

FIG. 4. Definition of the NF-κB2(p52) C-terminal cleavage site. (A) Mobilities of NF-κB2(p100), NF-κB2(p52), and truncated forms of NF-κB2 in denaturing SDS-PAGE. 293 cells were transfected with RSV expression plasmids terminated at the residues indicated above the lanes, and whole-cell lysates were separated on 8% denaturing gels prior to transfer to nitrocellulose and immunodetection with αp100N. Lane 1, full-length NF-κB2(p100) (899 residues); lanes 2 to 7, various deletions. Precursor (PRE), processed (PRO), and nonspecific (NS) bands are shown, with molecular weight markers (in thousands) indicated at the right. (B) Mobilities in SDS-PAGE of the constructs in gels similar to that shown in panel A, expressed as R_f values, plotted against the number of amino acid residues in each protein. Measurement of the distance migrated by p52 and interpolation on the graph (broken line) predicted Ala-405 as the C-terminal residue. The points plotted are the means from three separate determinations. (C) Amino acid sequence of NF-κB2 in the region of protease cleavage, showing the positions of artificially truncated proteins terminating at Ser-360, Pro-399, Ala-405, Gln-406, Glu-422, and Glu-445 (underlined). The predicted C-terminal residue of p52, Ala-405, is also indicated (arrow).

of p100 was replaced by a region of NF-κB1(p105) (Fig. 5A). The wild-type sequence in NF-κB2, PGGGGGA/QMAATVP (residues 399 to 412, with the slash indicating the C terminus of p52 at position 405), was replaced by PGTGTPGYSFPHYG in NF-κB2/1(400/401); however, the processed product remained the same (Fig. 5D, lane 2 versus lane 4), indicating that the glycine residue from NF-κB1 at position 405 of the fusion protein was likely to be the terminal residue. Hence, cleavage occurred at the same relative position in the protein regardless of the primary sequence at the processing site, and the sequence immediately surrounding Ala-405 was not required for degradation or for its termination at this site. In addition, the sequences around Ala-405 of NF-κB2 were altered to determine whether the primary sequence adjacent to the cleavage site affected the termination of processing; however, the P-399→A (P399A), G404A, A405P, and Q406N mutants were processed with unchanged kinetics and generated the expected products (data not shown).

While replacement of the NF-κB2 processing site with heterologous sequences from NF-κB1 supported the hypothesis that cleavage could occur regardless of the primary sequence, it remained possible that structural components from NF-κB1 could contribute to the processing. We therefore replaced the C terminus of NF-κB2(p100) with entirely heterologous sequences encoded by the bacterial *lacZ* gene. Fusion with LacZ sequences at residue 449, which removed the ankyrin repeats, or at residue 400, which removed both ankyrin repeats and the processing site, still resulted in the generation of a 52-kDa processed form (Fig. 5E, lanes 3 and 4). Hence, accurate processing can occur in the absence of any NF-κB sequences downstream of residue 400.

Stable dimer formation is required for effective proteolysis. One of the determinants encoded by the N-terminal portion of NF-κB2 is dimerization. Specific residues in both NF-κB1 (32) and RelB (44) which contribute to the dimerization interface have been identified. To determine whether formation of a stable dimer was required for accurate processing of NF-κB2, we mutated residues 247 to 249 (Tyr, Leu, and Leu) to alanine to generate the construct p100ΔDIM. The encoded protein failed to dimerize effectively through the RHD with a partner such as RelA (Fig. 6A). The ability to form a heterodimer with RelA was reduced ca. twofold; however, removal of the C-terminal domain of NF-κB2(p100) in this mutant resulted in a 20-fold reduction in dimerization capacity (data not shown), indicating that interaction through the RHD was disrupted but heterodimers are stabilized by the ankyrin repeat-containing portion of the molecule. Formation of p52 from p100ΔDIM was significantly reduced (Fig. 6A, lane 2, and B, lanes 9 to 12). In addition, p100ΔDIM was proteolyzed at a much higher rate (half-life of ~1 h) than the wild-type protein (half-life of >5 h) (Fig. 6B). Surprisingly degradation of p100ΔDIM was not inhibited by the proteasome inhibitor PSI at 25 μM, a concentration which completely inhibits generation of p52 from wild-type p100 (Fig. 6B, lanes 5 to 8 versus lanes 13 to 16). These findings suggest that dimerization, which is normally provided through the Rel-conserved domain, is required for stability of

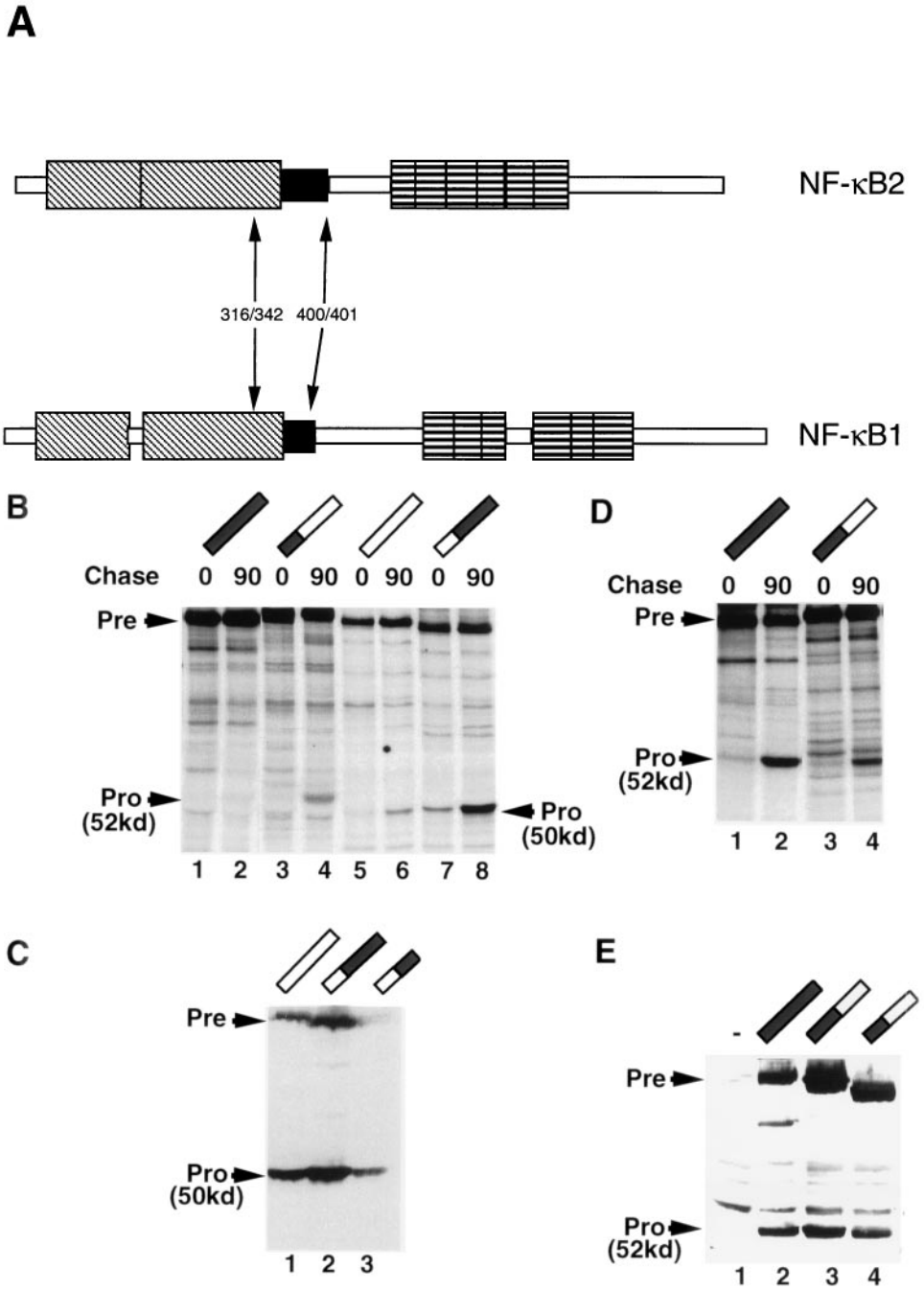

FIG. 5. Analysis of sequences required for accurate processing. (A) Schematic representation of constructs. NF-κB2(p100) and NF-κB1(p105) are shown aligned at the C terminus of the RHD (hatched). The glycine hinge (black) and ankyrin repeats (horizontal stripes) are also indicated; regions with poor primary sequence conservation are unshaded. The positions of swap constructs NF-κB2/1(316/342) and NF-κB2/1(400/401) are indicated. NF-κB1/2(342/318) is the converse swap to NF-κB2/1(316/342). (B) Processing of NF-κB precursor fusions. 293 cells were transfected with the constructs shown, and following metabolic labeling with [^{35}S]Met-Cys for 30 min followed by no chase (odd-numbered lanes) or a 90-min chase (even-numbered lanes), proteins were immunoprecipitated with αp100N (lanes 1 to 4) or αp105N (lanes 5 to 8). Precursor (Pre) and processed (Pro) forms are indicated. NF-κB2 sequences are shown by shading; NF-κB1 sequences are unshaded. The fusion proteins shown are NF-κB2/1(316/342) (lanes 3 and 4) and NF-κB1/2(342/318) (lanes 7 and 8). (C) Processing terminates at the same residue in NF-κB1/2(342/318) as in wild-type NF-κB2. 293 cells transfected with NF-κB1(p105), NF-κB1/2(342/318), or NF-κB1/2(405stop) (lanes 1 to 3, respectively) were lysed, and proteins were detected by Western blot analysis with αp105N. NF-κB1/2(405 stop) (lane 3) has the same mobility as the processed forms detected in lanes 1 and 2. (D) Analysis of the NF-κB2/1(400/401) chimera. Conditions were the same as for panel B. Lanes 1 and 2, wild-type p100; lanes 3 and 4, NF-κB2/1(400/401). (E) Cleavage of NF-κB2 fusions with heterologous C termini. NF-κB2 fusion proteins in which the C-terminal ankyrin repeat domain was replaced by the C-terminal 518 amino acids of the *E. coli* LacZ protein were generated. Cells transfected with a control plasmid, p100, p100(449)lacZ, or p100(400)lacZ (lanes 1 to 4, respectively) were lysed and analyzed by Western blotting with αp100N. Each precursor generated a 52-kDa processed form. NF-κB2 sequences are indicated by dark shading, and LacZ sequences are indicated by light shading.

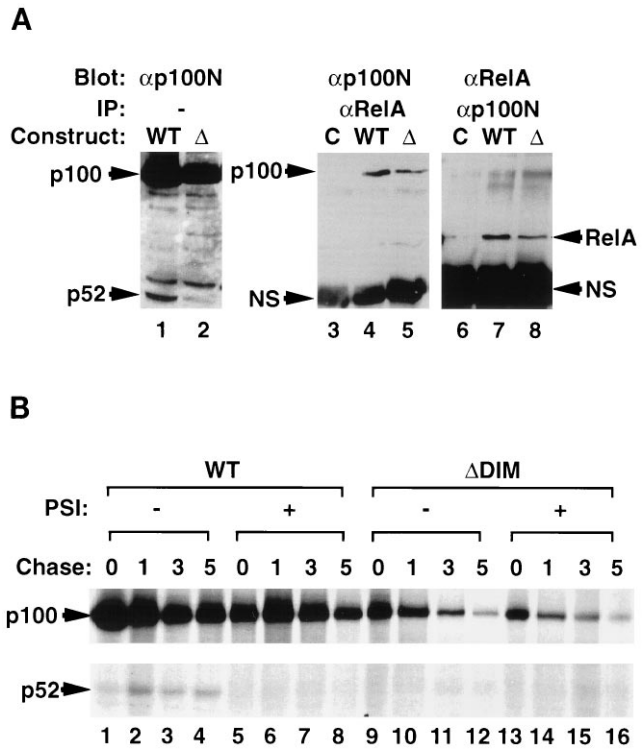

FIG. 6. Requirement of dimerization for effective processing. (A) Characterization of p100ΔDIM. Expression of p100ΔDIM (Δ) was compared with that of the wild-type (WT) protein following transfection into 293 cells and immunoblotting with αp100N (lanes 1 and 2). The ability to heterodimerize with RelA was tested in cells cotransfected with p100 constructs and RelA. Lysates were immunoprecipitated with αRelA (lanes 3 to 5) or αp100N (lanes 6 to 8), and complexes were analyzed by Western blotting with αp100N (lanes 3 to 5) or αRelA (lanes 6 to 8). p100ΔDIM showed a twofold reduction in the capacity to heterodimerize with RelA (lanes 4 and 7 versus lanes 5 and 8). NS, nonspecific cross-reactivity with the immunoglobulin used in immunoprecipitation (IP). C, control. (B) p100ΔDIM proteolysis is rapid but is not disrupted by proteasome inhibitors. 293 cells expressing wild-type or p100ΔDIM proteins were ^{35}S labeled and chased for the indicated times (in hours) in the absence (−) or presence (+) of 25 μM PSI.

NF-κB2, which is otherwise degraded through an independent pathway.

DISCUSSION

NF-κB2(p100) is structurally homologous to NF-κB1(p105) (4, 34, 46); however, its processed DNA binding form, NF-κB2(p52), has distinct functional properties. For example, this subunit of NF-κB shows altered affinity for distinct κB sites (14, 39). It also demonstrates more effective cooperativity with RelA in activation of the human immunodeficiency virus enhancer (46) and acts preferentially with Bcl-3 (5, 35). Hence, as a member of the Rel family of proteins, NF-κB2 provides a means to differentially regulate κB-dependent gene expression, on the basis of the different complexes. In this study, we have characterized the expression of NF-κB2(p100) and NF-κB2(p52) in different cell types and have examined the regulation of their proteolysis. We have found that NF-κB2(p100) was detectable in all cell lines studied and that protein levels were increased following activation of NF-κB, for example, by TNF-α. In B lymphocytes constitutive levels were high, presumably because of the constitutive presence of NF-κB in these cells. The *nfkb2* gene is transcriptionally activated by NF-κB complexes (28); hence, autoregulation of the *nfkb2* promoter allows stimulation of p100 by TNF-α in non-B-cell lines, and in B cells, enhanced degradation of IκB-α (31) increases its transcription.

In some cell lines, NF-κB2(p100) detected following immunoprecipitation was evident as a doublet in SDS-PAGE, and treatment with phosphatase or mutation of three serines at residues 713, 715, and 717 abolished the upper band. Recently, it has been shown that IκB-α is subject to phosphorylation in its C terminus by casein kinase II, and it is interesting that serines 713 and 715 fall within consensus sequences for this enzyme. Similar to the case for IκB-α (1), disruption of phosphorylation by mutation of these sites had no detectable effect on the rate of processing, but in contrast to the case for IκB-α, processing was insensitive to TPCK (Fig. 3B, lane 13). NF-κB2 (p100) is inducibly phosphorylated in HeLa cells following stimulation with TNF-α (33), and it is likely that this phosphorylation occurs on residues in addition to serines 713, 715, and 717. In contrast, in 293 cells, we found no alteration in the level of phosphorylation of p100 after TNF-α treatment (data not shown). In the study by Naumann and Scheidereit (33), constitutive phosphorylation of NF-κB2(p100) was detectable only in B cells. Our data indicated that the phosphorylation levels of p100 vary according to cell type, with the hyperphosphorylated form readily detectable in 293 cells and melanoma cells but not in other cell lines. In addition to 293 and UM-449 cells, we also detected constitutive phosphorylation in Jurkat T cells by P_i labeling (data not shown); however, a mobility shift in SDS-PAGE was not evident by ^{35}S labeling. Inducible phosphorylation regulates signal-mediated degradation of NF-κB1 (p105) and NF-κB2(p100) (13, 29, 30). It therefore appears that two distinct phosphorylation events, one constitutive and one inducible, occur in NF-κB2(p100). Phosphorylation events are also cell line specific and potentially contribute to differential regulation of NF-κB family members. Although similar to that of IκB-α in some respects, the lack of inhibition by TPCK or related inhibitors suggests that distinct kinases are involved in NF-κB2 and IκB-α proteolysis. Some studies have shown increased levels of p52 following cellular stimulation (30), and recent results show similar effects for NF-κB1 in the presence of Tax (43). In our study, we were unable to detect significant increases in the processing of NF-κB2 following treatment with agonists such as TNF-α. The increases seen in the earlier studies may have been caused by increased transcription and translation of NF-κB seen at later times after induction.

NF-κB precursors are unusual in their regulation by the proteasomal pathway in that proteolysis terminates at a site within the molecule and does not lead to complete protein degradation. This controlled degradation could be due to the presence of a specific stop signal or other structural determinants in the N-terminal half of NF-κB2(p100) which dictate the site of cleavage. While the predicted C-terminal amino acid of NF-κB2(p52) was defined as alanine 405 by deletion analysis, deletion or mutation of this residue or surrounding residues did not affect the size of the processed product, indicating that a specific sequence motif at the cleavage site was not required. Proteolysis occurred at the same relative position in the molecule regardless of the primary sequence immediately downstream of the glycine hinge. It is unlikely that an independent cleavage sequence from p105 determined the proteolysis in the NF-κB2/NF-κB1 fusions, as the relative position of such a sequence motif would be altered in these proteins, being 26 residues more N terminal in NF-κB2/NF-κB1(316/342) compared with NF-κB2/NF-κB1(400/401), and would be expected to generate products with different molecular weights. Furthermore, NF-κB1 and NF-κB2 apparently have similar

mechanisms of processing but lack sequence homology in the region C terminal to the glycine hinge which defines the C termini of both processed forms. The lack of a primary sequence requirement at the position of cleavage was further supported by replacement of the entire C terminus and processing site of NF-κB2 with heterologous sequences, which also resulted in the generation of p52. We concluded that a specific sequence motif was not required in this domain of the molecule. Rather, the limits of processing were defined by structural determinants in the N-terminal region. These data are consistent with a recent report by Lin and Ghosh (25), who demonstrated the importance of the glycine-rich region of NF-κB1 as a processing signal sequence for p105. The sequence of the cleavage site in their study was also found not to determine the position of cleavage, and transposition of the glycine-rich domain to an unrelated protein was able to stimulate processing of heterologous proteins unrelated to NF-κB (25), presumably mediated by the proteasome.

The proteasome is a 700-kDa complex comprising 28 subunits arranged as a stack of four heptameric rings with the center forming a catalytic core (reviewed in reference 19). Cleavage of target proteins can occur at the C-terminal side of hydrophobic, basic, and acidic residues (chymotryptic, tryptic, and peptidylglutamyl activities, respectively), and the specificity of cleavage is determined by the subunits incorporated into the proteasome. For example, inclusion of LMP2 and LMP7 subunits increases cleavage following hydrophobic residues (18). We demonstrated inhibition of NF-κB2(p100) processing by using a specific inhibitor of the chymotrypsin-like activity of the proteasome (58), which has previously been shown to prevent IκB-α degradation (53). We did not directly demonstrate attachment of ubiquitin to the NF-κB2(p100) C terminus, as the α-ubiquitin antibodies that we tested did not efficiently detect the ligated form; however, multiubiquitination of both NF-κB1(p105) and IκB-α has been demonstrated (8, 37), and it is expected that the same mechanism operates for NF-κB2. Recent in vitro evidence has demonstrated a role for a ubiquitin-conjugating system comprising the ubiquitin carrier protein E2-F1 and a novel ubiquitin-protein ligase in proteolysis of NF-κB1(p105) (36), and the Ubc4/Ubc5 family of E2 proteins ubiquitinate IκBα (9). While the processing pathways for the NF-κB1 and NF-κB2 precursors are analogous, there was a clear quantitative difference in 293 cells between the amounts of p50 and p52 generated. Furthermore, while the processing of both NF-κB1 and NF-κB2 was inhibited by peptide aldehyde inhibitors of the proteasome, NF-κB2 proteolysis was more sensitive to these compounds. Because both precursor molecules are expressed widely and at comparable levels, this difference in processing may explain the lower levels of p52 found in most cells studied, where NF-κB1(p50) is the predominant subunit found heterodimerized with other Rel family members. Such differential processing may allow for selective generation of specific combinations of subunit heterodimers. NF-κB2(p100) proteolysis may be elevated in other cell types or at different stages of cellular development. In this respect, it is notable that whereas NF-κB1(p50) is detected in virtually all cell lines, NF-κB2(p52) is expressed more selectively, for example, in H9 T cells, Raji cells, and Daudi B cells, all of which contain constitutive NF-κB in the nucleus (6, 12). NF-κB2 (p52) is detected at later stages of B-cell development but not immediately following a mitogenic stimulus (27). Our data therefore suggest a temporal mechanism for controlling the transcriptional response at the level of NF-κB precursors and differential proteolytic processing among NF-κB and IκB family members which allows for the generation of specific active complexes following cellular stimulation.

ACKNOWLEDGMENTS

We thank Donna Gschwend for secretarial assistance, Nancy Barrett and Karen Carter for assistance with figures, S. Wilk and N. Rice for the generous contribution of reagents, and A. L. Goldberg, O. Coux, and S. Ghosh for helpful discussions. The contributions of N. Perkins and other members of the Nabel laboratory are also appreciated.

REFERENCES

1. **Barroga, C. F., J. K. Stevenson, E. M. Schwarz, and I. M. Verma.** 1995. Constitutive phosphorylation of IκBα by casein kinase II. Proc. Natl. Acad. Sci. USA **92:**7637–7641.
2. **Beg, A. A., W. C. Sha, R. T. Bronson, and D. Baltimore.** 1995. Constitutive NF-κB activation, enhanced granulopoiesis, and neonatal lethality in IκBα-deficient mice. Genes Dev. **9:**2736–2746.
3. **Beg, A. A., W. C. Sha, R. T. Bronson, S. Ghosh, and D. Baltimore.** 1995. Embryonic lethality and liver degeneration in mice lacking the RelA component of NF-κB. Nature (London) **376:**167–170.
4. **Bours, V., P. R. Burd, K. Brown, J. Villalobos, S. Park, R. Ryseck, R. Bravo, K. Kelly, and U. Siebenlist.** 1992. A novel mitogen-inducible gene product related to p50/p105-NF-κB participates in transactivation through a κB site. Mol. Cell. Biol. **12:**685–695.
5. **Bours, V., G. Franzoso, V. Azarenko, S. Park, T. Kanno, K. Brown, and U. Siebenlist.** 1993. The oncoprotein Bcl-3 directly transactivates through κB motifs via association with DNA-binding p50B homodimers. Cell **72:**729–739.
6. **Brown, A. M., M. W. Linhoff, B. Stein, K. L. Wright, A. S. Baldwin, Jr., P. V. Basta, and J. P. Y. Ting.** 1994. Function of NF-κB/Rel binding sites in the major histocompatibility complex class II invariant chain promoter is dependent on cell-specific binding of different NF-κB/Rel subunits. Mol. Cell. Biol. **14:**2926–2935.
7. **Brown, K., S. Gerstberger, L. Carlson, G. Franzoso, and U. Siebenlist.** 1995. Control of IκB-α proteolysis by site-specific, signal-induced phosphorylation. Science **267:**1485–1488.
8. **Chen, Z., J. Hagler, V. J. Palombella, F. Melandri, D. Scherer, D. Ballard, and T. Maniatis.** 1995. Signal-induced site-specific phosphorylation targets IκBα to the ubiquitin-proteasome pathway. Genes Dev. **9:**1586–1597.
9. **Chen, Z. J., L. Parent, and T. Maniatis.** 1996. Site-specific phosphorylation of IκBα by a novel ubiquitination-dependent protein kinase activity. Cell **84:**853–862.
10. **Ciechanover, A.** 1994. The ubiquitin-proteasome proteolytic pathway. Cell **79:**13–21.
11. **DiDonato, J. A., F. Mercurio, and M. Karin.** 1995. Phosphorylation of IκB-α precedes but is not sufficient for its dissociation from NF-κB. Mol. Cell. Biol. **15:**1302–1311.
12. **Dobrzanski, P., R. Ryseck, and R. Bravo.** 1994. Differential interactions of Rel-NF-κB complexes with IκBα determine pools of constitutive and inducible NF-κB activity. EMBO J. **13:**4608–4616.
13. **Donald, R., D. W. Ballard, and J. Hawiger.** 1995. Proteolytic processing of NF-κB/IκB in human monocytes. J. Biol. Chem. **270:**9–12.
14. **Duckett, C. S., N. D. Perkins, T. F. Kowalik, R. M. Schmid, E. S. Huang, A. S. Baldwin, Jr., and G. J. Nabel.** 1993. Dimerization of NF-KB2 with RelA(p65) regulates DNA binding, transcriptional activation, and inhibition by an IκB-α (MAD-3). Mol. Cell. Biol. **13:**1315–1322.
15. **Figueiredo-Pereira, M. E., K. A. Berg, and S. Wilk.** 1994. A new inhibitor of the chymotrypsin-like activity of the multicatalytic proteinase complex (20S proteasome) induces accumulation of ubiquitin-protein conjugates in a neuronal cell. J. Neurochem. **63:**1578–1581.
16. **Finco, T. S., A. A. Beg, and A. S. Baldwin, Jr.** 1994. Inducible phosphorylation of IκBα is not sufficient for its dissociation from NF-κB and is inhibited by protease inhibitors. Proc. Natl. Acad. Sci. USA **91:**11884–11888.
17. **Gaczynska, M., K. L. Rock, and A. L. Goldberg.** 1993. Gamma-interferon and expression of MHC genes regulate peptide hydrolysis by proteasomes. Nature (London) **365:**264–267.
18. **Gaczynska, M., K. L. Rock, T. Spies, and A. L. Goldberg.** 1994. Peptidase activities of proteasomes are differentially regulated by the major histocompatibility complex-encoded genes for LMP2 and LMP7. Proc. Natl. Acad. Sci. USA **91:**9213–9217.
19. **Goldberg, A. L.** 1995. Functions of the proteasome: the lysis at the end of the tunnel. Science **268:**522–523.
20. **Henkel, T., T. Machleidt, I. Alkalay, M. Kronke, Y. Ben-Neriah, and P. A. Baeuerle.** 1993. Rapid proteolysis of IκB-α is necessary for activation of transcription factor NF-κB. Nature (London) **365:**182–185.
21. **Henkel, T., U. Zabel, K. van Zee, J. M. Muller, E. Fanning, and P. A. Baeuerle.** 1992. Intramolecular masking of the nuclear location signal and dimerization domain in the precursor for the p50 NF-κB subunit. Cell **68:**1121–1133.
22. **Ip, Y. T., M. Reach, Y. Engstrom, L. Kadalayil, H. Cai, S. Gonzalez-Crespo, K. Tatei, and M. Levine.** 1993. Dif, a dorsal-related gene that mediates an immune response in Drosophila. Cell **75:**753–763.
23. **Jensen, T. J., M. A. Loo, S. Pind, D. B. Williams, A. L. Goldberg, and J. R. Riordan.** 1995. Multiple proteolytic systems, including the proteasome, con-

tribute to CFTR processing. Cell **83:**129–135.
24. **Kontgen, F., R. J. Grumont, A. Strasser, D. Metcalf, R. Li, D. Tarlinton, and S. Gerondakis.** 1995. Mice lacking the c-rel proto-oncogene exhibit defects in lymphocyte proliferation, humoral immunity, and interleukin-2 expression. Genes Dev. **9:**1965–1977.
25. **Lin, L., and S. Ghosh.** 1996. A glycine-rich region in NF-κB p105 functions as a processing signal for the generation of the p50 subunit. Mol. Cell. Biol. **16:**2248–2254.
26. **Liou, H. C., G. P. Nolan, S. Ghosh, T. Fujita, and D. Baltimore.** 1992. The NF-kappa B p50 precursor, p105, contains an internal I kappa B-like inhibitor that preferentially inhibits p50. EMBO J. **11:**3003–3009.
27. **Liou, H. C., W. C. Sha, M. L. Scott, and D. Baltimore.** 1994. Sequential induction of NF-κB/Rel family proteins during B-cell terminal differentiation. Mol. Cell. Biol. **14:**5349–5359.
28. **Liptay, S., R. M. Schmid, E. G. Nabel, and G. J. Nabel.** 1994. Transcriptional regulation of NF-κB2: evidence for κB-mediated positive and negative autoregulation. Mol. Cell. Biol. **14:**7695–7703.
29. **Mellits, K. H., R. T. Hay, and S. Goodbourn.** 1993. Proteolytic degradation of MAD3 (IκB-α) and enhanced processing of the NF-κB precursor p105 are obligatory steps in the activation of NF-κB. Nucleic Acids Res. **21:**5059–5066.
30. **Mercurio, F., J. A. DiDonato, C. Rosette, and M. Karin.** 1993. p105 and p98 precursor proteins play an active role in NF-κB-mediated signal transduction. Genes Dev. **7:**705–718.
31. **Miyamoto, S., P. J. Chiao, and I. M. Verma.** 1994. Enhanced IκB-α degradation is responsible for constitutive NF-κB activity in mature murine B-cell lines. Mol. Cell. Biol. **14:**3276–3282.
32. **Muller, C. W., F. A. Rey, M. Sodeoka, G. L. Verdine, and S. C. Harrison.** 1995. Structure of the NF-κB B p50 homodimer bound to DNA. Nature (London) **373:**311–317.
33. **Naumann, M., and C. Scheidereit.** 1994. Activation of NF-κB *in vivo* is regulated by multiple phosphorylations. EMBO J. **13:**4597–4607.
34. **Neri, A., C. C. Chang, L. Lombardi, M. Salina, P. Corradini, A. T. Maiolo, R. S. K. Chaganti, and R. Dalla-Favera.** 1991. B cell lymphoma-associated chromosomal translocation involves candidate oncogene, lyt-10, homologous to NF-κB p50. Cell **67:**1075–1087.
35. **Nolan, G. P., T. Fujita, K. Bhatia, C. Huppi, H. Liou, M. L. Scott, and D. Baltimore.** 1993. The bcl-3 proto-oncogene encodes a nuclear IκB-like molecule that preferentially interacts with NF-κB p50 and p52 in a phosphorylation-dependent manner. Mol. Cell. Biol. **13:**3557–3566.
36. **Orian, A., S. Whiteside, A. Israel, I. Stancovski, A. L. Schwartz, and A. Ciechanover.** 1995. Ubiquitin-mediated processing of NF-κB transcriptional activator precursor p105. J. Biol. Chem. **270:**21707–21714.
37. **Palombella, V. J., O. J. Rando, A. L. Goldberg, and T. Maniatis.** 1994. The ubiquitin-proteasome pathway is required for processing the NF-κB1 precursor protein and the activation of NF-κB. Cell **78:**773–785.
38. **Perkins, N. D., A. B. Agranoff, E. Pascal, and G. J. Nabel.** 1994. An interaction between the DNA-binding domains of RelA(p65) and Sp1 mediates human immunodeficiency virus gene activation. Mol. Cell. Biol. **14:**6570–6583.
39. **Perkins, N. D., R. M. Schmid, C. S. Duckett, K. Leung, N. R. Rice, and G. J. Nabel.** 1992. Distinct combinations of NF-κB subunits determine the specificity of transcriptional activation. Proc. Natl. Acad. Sci. USA **89:**1529–1533.
40. **Pines, J.** 1994. Ubiquitin with everything. Nature (London) **371:**742–743.
41. **Rice, N. R., M. L. MacKichan, and A. Israel.** 1992. The precursor of NF-κB p50 has IκB-like functions. Cell **71:**243–253.
42. **Rock, K. L., C. Gramm, L. Rothstein, K. Clark, R. Stein, L. Dick, D. Hwang, and A. L. Goldberg.** 1994. Inhibitors of the proteasome block the degradation of most cell proteins and the generation of peptides presented on MHC class I molecules. Cell **78:**761–771.
43. **Rousset, R., C. Desbois, F. Bantignies, and P. Jalinot.** 1996. Effects on NF-κB1/p105 processing of the interaction between the HTLV-1 transactivator Tax and the proteasome. Nature (London) **381:**328–331.
44. **Ryseck, R. P., J. Novotny, and R. Bravo.** 1995. Characterization of elements determining the dimerization properties of RelB and p50. Mol. Cell. Biol. **15:**3100–3109.
45. **Schmid, R. M., S. Liptay, J. C. Betts, and G. J. Nabel.** 1994. Structural and functional analysis of NF-κB: determinants of DNA binding specificity and protein interaction. J. Biol. Chem. **269:**32162–32167.
46. **Schmid, R. M., N. D. Perkins, C. S. Duckett, P. C. Andrews, and G. J. Nabel.** 1991. Cloning of an NF-κB subunit which stimulates HIV transcription in synergy with p65. Nature (London) **352:**733–736.
47. **Sha, W. C., H. C. Liou, E. I. Tuomanen, and D. Baltimore.** 1995. Targeted disruption of the p50 subunit of NF-κB leads to multifocal defects in immune responses. Cell **80:**321–330.
48. **Siebenlist, U., G. Franzoso, and K. Brown.** 1994. Structure, regulation and function of NF-κB. Annu. Rev. Cell. Biol. **10:**405–455.
49. **Steward, R.** 1987. Dorsal, an embryonic polarity gene in Drosophila, is homologous to the vertebrate proto-oncogene, c-rel. Science **238:**692–694.
50. **Thanos, D., and T. Maniatis.** 1995. NF-κB: a lesson in family values. Cell **80:**529–532.
51. **Thompson, J. E., R. J. Phillips, H. Erdjument-Bromage, P. Tempst, and S. Ghosh.** 1995. IκB-β regulates the persistent response in a biphasic activation of NF-κB. Cell **80:**573–582.
52. **Traenckner, E. B., H. L. Pahl, T. Henkel, K. N. Schmidt, S. Wilk, and P. A. Baeuerle.** 1995. Phosphorylation of human IκB-α on serines 32 and 36 controls IκB-α proteolysis and NF-κB activation in response to diverse stimuli. EMBO J. **14:**2876–2883.
53. **Traenckner, E. B., S. Wilk, and P. A. Baeuerle.** 1994. A proteasome inhibitor prevents activation of NF-κB and stabilizes a newly phosphorylated form of IκB-α that is still bound to NF-κB. EMBO J. **13:**5433–5441.
54. **Treier, M., L. M. Staszewski, and D. Bohmann.** 1994. Ubiquitin-dependent c-Jun degradation *in vivo* is mediated by the delta domain. Cell **78:**787–798.
55. **Ward, C. L., S. Omura, and R. R. Kopito.** 1995. Degradation of CFTR by the ubiquitin-proteasome pathway. Cell **83:**121–127.
56. **Weih, F., D. Carrasco, S. K. Durham, D. S. Barton, C. A. Rizzo, R. P. Ryseck, S. A. Lira, and R. Bravo.** 1995. Multiorgan inflammation and hematopoietic abnormalities in mice with a targeted disruption of RelB, a member of the NF-κB/Rel family. Cell **80:**331–340.
57. **Whiteside, S. T., M. K. Ernst, O. LeBail, C. Laurent-Winter, N. Rice, and A. Israel.** 1995. N- and C-terminal sequences control degradation of MAD3/IκB-α in response to inducers of NF-κB activity. Mol. Cell. Biol. **15:**5339–5345.
58. **Wilk, S., and M. E. Figueiredo-Pereira.** 1993. Synthetic inhibitors of the multicatalytic proteinase complex (proteasome). Enzyme Protein **47:**306–313.
59. **Zhuo, S., J. C. Clemens, D. J. Hakes, D. Barford, and J. E. Dixon.** 1993. Expression, purification, crystallization, and biochemical characterization of a recombinant protein phosphatase. J. Biol. Chem. **268:**17754–17761.